

A Numerical Analysis of Novel Liquid-Gas Jet Ejector

**Karthick Palani¹, Sarangapani Palani², Prabakaran Venkatakrishnan³,
Gurumurthy Veerapatharan³, Mohammed Raffe Rahamathullah⁴,
Kalaiselvane Adhimoulame⁵**

¹Assistant Professor, Department of Mechanical Engg. SKP Institute of Technology, Tiruvannamalai, India

²Assistant Professor, Department of Mechanical Engg. V.R.S.College of Engg.& Technology, Tamilnadu, India

³Assistant Professor, Department of Mechanical Engg. Dr.S.J.S.Paul Memorial college of Technology,
Pondicherry, India

⁴Department of Mechanical Engg. Pondicherry Engineering College, Pondicherry, India

⁵Associate Professor, Department of Mechanical Engg. Pondicherry Engineering College, Pondicherry, India

Abstract

In this article, numerical investigations have been carried out on ejectors employing liquid as a motive fluid and air as the entrained fluid. A numerical model has been developed to predict the air entrainment rate taking into account: (i) the compressible nature of air, (ii) pressure drop for two-phase flow and (iii) losses due to changes in cross sectional area. The effects of gas velocity, liquid level in the suction chamber, nozzle diameter and throat diameter on the liquid entrainment, entrainment ratio (L/G), pressure drop, gas hold-up, mass transfer coefficient and interfacial area have been investigated. The simulated performance is compared with the available experimental data from the literature for validation. The entrainment rate predicted from the numerical model shows good agreement with the experimental values.

I. Introduction

Ejectors are co-current flow systems, where simultaneous aspiration and dispersion of the entrained fluid takes place. This causes continuous formation of fresh interface and generation of large interfacial area because of the entrained fluid between the phases. The ejector essentially consists of an assembly comprising of nozzle, converging section, mixing tube/throat and diffuser. According to the Bernoulli's principle, when a motive fluid is pumped through the nozzle of a gas-liquid ejector at a high velocity, a low pressure region is created just outside the nozzle. A second fluid gets entrained into the ejector through this low pressure region. The dispersion of the entrained fluid in the throat of the ejector with the motive fluid jet emerging from the nozzle leads to intimate mixing of the two phases. A diffuser section after the mixing tube/throat helps in the pressure recovery. The motive fluid jet performs two functions; one, it develops the suction for the entrainment of the secondary fluid and the second: it provides energy for the dispersion of one phase into the other. This process has largely been exploited in

vacuum systems in which a high speed fluid stream (typically steam) is used to generate vacuum.

Ejectors also produce higher mass transfer rates by generating very small bubbles/droplets of the dispersed phase, thereby improving the contact between phases, which can then be injected into a reaction vessel [1]. Compared to the other gas-liquid contacting systems like stirred tanks and bubble columns, ejectors provide higher values of volumetric mass transfer coefficient [2,3]. In chemical industries, ejectors are also used to entrain and pump corrosive liquids, slurries, fumes and dust-laden gases, which otherwise are difficult to handle [4]. Jet ejectors can also be used for mass transfer operations like gas absorption or stripping [5]. High values of mass transfer coefficient and interfacial area enable a substantial reduction in the size (and hence capital cost) of a mass transfer contactor. The benefits are particularly important if the intrinsic rates of chemical reactions accompanying the mass transfer operations are very high and a mass transfer controlled regime prevails. For example, in the chemical exchange process producing heavy water [6], a synthesis gas mixture of nitrogen and hydrogen is contacted with liquid ammonia at high pressure and low temperature conditions. The deuterium absorption from the gas mixture into the liquid ammonia takes place in the presence of KNH_2 as a catalyst. Deuterium is present in gaseous hydrogen as HD at a concentration of about 100 ppm. HD dissolves into the liquid phase and reacts with ammonia to form deuterated ammonia. The rate of this isotopic exchange reaction in the presence of KNH_2 is very fast as compared to the gas-liquid mass transfer rate (at the temperature and catalyst concentration employed on the industrial scale). The rate of mass transfer, therefore, becomes the controlling step in the overall process. To achieve higher mass transfer rates, on each tray of the exchange towers, a large number of ejectors are provided. The use of ejector trays substantially reduces the size of the column required for the operation. To design such gas-liquid contactors, it is

necessary to establish quantitative relationships between geometry of the ejector, the operating conditions and the performance of the ejector. The important design parameters for such contactors are entrainment rate, pressure drop across the entire length, hold-up of the phases and mass transfer characteristics within the ejector. A majority of the published literature on ejectors deals broadly with the design and performance of steam and liquid-jet ejectors. The reported work on gas-liquid jet ejectors with gas as the motive fluid and liquid as the entrained fluid is scanty. Therefore, studies were undertaken to investigate hydrodynamic and mass transfer characteristics of gas-liquid ejectors with gas as the motive fluid. Based on the flow direction, three types of ejectors have been reported, viz., vertical up-flow, vertical down-flow and horizontal flow. Several authors have performed detailed experiments with all the three types of ejectors and have developed numerous correlations to predict the entrainment rate, gas holdup, mass transfer coefficient and interfacial area, empirically. In the following section, the literature on entrainment rate (in terms of mass ratio), hold-up and mass transfer parameters has been analyzed first. It should be noted that almost all the correlations reported by various authors in the following section employ liquid as primary fluid and gas as secondary fluid.

A number of researchers have developed correlations for their respective geometries using dimensional analysis (Table 1). Most of these correlations are similar but vary widely in the exponents of different terms. For example, the exponent of area ratio varies from 0.07 [10] to 0.68 [4]. Bhutada and Pangarkar [10] reported four different correlations, one each for four throats investigated by them. These correlations are highly specific to the nozzle-throat geometry and thus cannot be generalized. Various authors [4, 5, 8, 11-14] have attempted to predict the entrainment rate based on momentum and energy balances across different sections of the ejector. Table 2 shows the geometry of ejectors and the respective correlations obtained through such analysis as available in literature. All the authors have applied a mechanical energy balance to account for the changes in the cross sectional area of an ejector and a momentum balance across the straight sections of the ejector. The empiricism in their work comes from: (i) fitted loss coefficient, K' , (ii) the pressure recovery factor, β and (iii) the correlation between K' and β . From the analysis of the previous work, it can be said that the relationships for mass ratio predictions are semi empirical and depend on the geometry, fluid property, operating conditions. Mandal et al. [14] assumed that the entrained gas as ideal and isothermal. The energy loss coefficient across the nozzle was obtained from the energy balance.

1.1 Mass Ratio

Table 1
Mass ratio correlations from dimensionless analysis given by various authors

Primary fluid	Secondary fluid	Geometry and range investigated	Mass ratio correlation	Authors
Air	Water	Flow—upward: $D_N = 0.00808-0.002676$ m, $D_T = 0.0127$ m, $H_T = 0.0889$ m, $(D_N/D_T) = 0.009-0.2107$, $D_C = 0.0635$ m, $H_C = 1.219$ m	$M_r = k \left(\frac{\mu_m}{D_N \rho_m U_m} \right)^{0.76} (A_r)^{0.4} \left(\frac{g \mu_m^4}{\rho_e \sigma_e^2} \right)^{-0.04} \left(\frac{\rho_e - \rho}{\rho_e} \right)^{0.63}$	[7]
Water, glycerine, kerosene	Air	Flow—horizontal: $D_N = 0.0019-0.00449$ m, $D_T = 0.00925$ m, $D_N/D_T = 0.2-0.48$, $H_T = 0$, $D_C = 0.0254$ m, $H_C = 1.1$ m	$M_r = 8.5 \times 10^{-2} \left(\frac{\Delta P}{\rho_e U_e^2} \right)^{-0.3} (A_r)^{0.46} \left(\frac{g \mu_m^4}{\rho_m \sigma_m^2} \right)^{-0.02}$	[8]
Water, glycerine, kerosene	Air	Flow—upward: $D_N = 0.00178-0.0055$ m, $D_T = 0.0127$ m, $H_T = 0.1016$ m, $D_N/D_T = 0.14-0.433$	$M_r = 5.2 \times 10^{-4} \left(\frac{\Delta P}{\rho_e U_e^2} \right)^{-0.305} (A_r)^{0.68} \left(\frac{g \mu_m^4}{\rho_m \sigma_m^2} \right)^{-0.305}$	[4]
Water, mono ethylene glycol	Air	Flow—downward: $D_N = 0.0025$ m, $D_T = 0.005$ m, $H_T = 0.0175$, $D_N/D_T = 0.5$, $H_C = 1$ m, $D_C = 0.01$ m	$M_r = 43.86 \times 10^{-3} \left(\frac{\Delta P}{\rho_e U_e^2} \right)^{-0.38} \left(\frac{g \mu_m^4}{\rho_m \sigma_m^2} \right)^{-0.01}$	[5]
Water	Air	Flow—downward: $D_N = 0.0045, 0.0065$ m, $D_T = 0.018$ m, $D_C = 0.040$ m	$M_r = 2.4 \times 10^{-3} \left(\frac{\Delta P}{\rho_e U_e^2} \right)^{-0.82} \left(\frac{g \mu_m^4}{\rho_m \sigma_m^2} \right)^{-0.01}$	[9]
Water	Air	Flow—downward: $D_N = 0.005, 0.008, 0.01, 0.012$ m, $D_T = 0.016, 0.0159$ m, $D_N/D_T = 1.6-3.2$	$M_r = x \left(\frac{\Delta P}{\rho_e U_e^2} \right)^y (A_r)^z$; $x = 5.58 \times 10^{-4}$ to 9.67×10^{-4} ; $y = -0.135$ to -0.202 ; $z = 0.07-0.224$	[10]

The pressure energy, kinetic energy and energy dissipation per unit mass of the liquid and gas were considered in the energy balance. No mixing was assumed in throat and diffuser and hence all the energy losses were only the frictional losses. The values of K_{ejt} can be back calculated from the ejector efficiency data given by ref. [14]. The values of K_{ejt} were in the range 0.06–0.1 for various geometries

investigated by the authors. This means that the contributions of the work for the gas compression and the hydrostatic head are very small. Some of the previous models reported by refs [5, 13, 14] take the compressibility of air into account. But all these models were developed for liquid as the motive fluid and the gas as the entrained fluid.

Table 2. Mass ratio correlations from theoretical analysis given by various authors.

Authors	Geometry and range investigated	Geometry and the locations where the energy and momentum balance were taken	Correlation and remarks on loss coefficient
Bhat <i>et al.</i> (1972)	Flow—horizontal $D_N = 0.0019-0.00449$, $D_T = 0.00925$, $D_N/D_T = 0.2-0.48$, $H_T = 0$, $D_C = 0.0254$, $H_C = 1.1$. Primary fluid—water, glycerine and kerosene. Secondary fluid—air Maximum L/G = 60		$M_2^2 \rho_2 \left[-\gamma_2^2 + \frac{2\gamma_1 A_V}{(A_V - 1)} + 2(\gamma_1 - 1) \left(\frac{\gamma_3}{\gamma_3 - 1} \right) \left(\gamma_3 - \frac{A_V}{A_V - 1} \right) - \gamma_1^2 \right] - M_1 \gamma_1^2 (\rho_1 + 1) - (\beta + K') A_V^2 + 2\gamma_1 A_V - (\gamma_1^2 + \gamma_2^2) = 0$ All the losses are clubbed as loss factor K' and values of K' were fitted using experimental results K' was empirically fitted to β and A_e $K' = -\beta - 0.0123A_V + 0.116$ Each area ratio has different K' and the value ranges from 0.01 to 0.05
Acharjee <i>et al.</i> (1975)	Flow—upward $D_N = 0.00178-0.0055$, $D_T = 0.0127$, $H_T = 0.1016$ $D_N/D_T = 0.14-0.433$ Primary fluid—water, glycerine, kerosene Secondary fluid—air		$M_2^2 \rho_2 \left[\gamma_2^2 + \frac{A_V(A_V - 2)}{(A_V - 1)^2} - 1 \right] - M_1 (\rho_1 + 1) + 2A_V - (K' + \beta) A_V^2 - 1 = 0$ All the losses are clubbed as loss factor K' and was fitted to match the experimental values $K' = -0.82\beta + \frac{1.52}{0.95A_V}$ Each area ratio has different K' and value ranges from 0.01 to 0.28

Table 2 (Continued)

Geometry and range investigated	Geometry and the locations where the energy and momentum balance were taken	Correlation and remarks on loss coefficient	Authors
Secondary fluid—air Maximum L/G = 14 Flow—horizontal: review of existing data, single phase		$M_2^2 = \frac{K_2 \rho_2}{\rho_m} \left[K' \gamma_2^2 + K_1 \gamma_2^2 + \frac{4f_s H_T}{D_T} + \frac{4f_s H_C \gamma_2^2}{D_C} + (1 + K_D)(1 - \gamma_2)^2 \right]$ K_2 and n are fitted from experimental data Total loss coefficient = 1 - diffuser efficiency + loss coefficient of throat $P_3 - P_{03} = \frac{\rho_m U_m^2}{2} \left[\frac{2}{A_e} \left(\frac{M_2^2 \rho_2}{A_e} + 1 \right) - \frac{M_2^2 \rho_2}{(A_e - 1)^2} (1 - K_N) - \frac{(1 + M_2)(M_2 \rho_2 + 1)}{A_e^2} (1 + K_1) \right]$ K_1 and K_N were obtained from experimental data of previous authors also single loss coefficient was proposed. Value of K' ranges from 0.21 to 0.34	[12]
Flow—downward: $D_N = 0.0025$, $D_T = 0.005$, $H_T = 0.0175$, $D_N/D_T = 0.5$, $H_C = 1$, $D_C = 0.01$ Primary fluid—water, mono ethylene glycol Secondary fluid—air Maximum L/G = 15		$M_1^2 \rho_1 \left[\gamma^2 \frac{A_e^2}{A_e} + \frac{A_e(A_e - 2)}{(A_e - 1)^2} \right] + 2A_e + \frac{1 + M_2}{M_2 \rho_2 (1 + \epsilon) + 1} + [2A_e^2 Fr - M_1 \rho_1 (\epsilon + 1) - (K'' + \beta) A_e^2] = 0$ $K'' = -1.11\beta + 0.445$ All the losses are clubbed as loss factor K' and was fitted with experimental values. Values of K' ranges from 3–7	[5]

1.2 Fractional Gas Hold-Up

Table 3 shows the geometry of the ejectors, methods of gas hold-up measurement and the correlations as available in literature. The gas hold-up was correlated to ejector geometry, gas entrainment rate and energy dissipation per unit volume. The form of most of these correlations is similar but with a wide variation in the exponents of different terms. For example, the exponent of gas velocity varies from 0.55 [18] to 1.08 [25]. These correlations are

highly specific to particular nozzle–throat geometry. Zahradnik *et al.* [2, 16, 17, 19, 20] in a series of papers have reported the use of ejector-type gas distributors for the gas–liquid contacting in bubble columns. They have reported that an ejector acts as a gas distributor that allows gas to be entrained into the bubble column rather than sparged. The gas–liquid contact is first achieved in the ejector and subsequently, the flow pattern generated in the bubble column produces good mixing of the gas and the liquid phases. It was reported that for a given

superficial gas velocity, higher fractional gas hold-up was observed with the ejector distributor than that with a conventional sieve plate distributor. The gas hold-up was further correlated empirically with the superficial velocity of the gas. The gas hold-up varied linearly with the superficial velocity of the entrained gas, i.e. $\epsilon_G = 3.47V_G$, in contrast to less than linear variation of fractional gas hold-up using sieve tray distributor, i.e. $\epsilon_G = 0.74V_G^{0.6}$. Dutta and Raghavan [9] have correlated the gas hold-up in the vessels empirically with the specific power consumption (P/V_L) in the vessel. Bhutada and Pangarkar [10] have studied the effect of diffuser type on the gas hold-up. Bhutada and Pangarkar [10] have shown that the gas hold-up is a strong function of the gas

entrainment rate and a relatively weak function of the geometry of the ejector. They have developed correlation for predicting the gas hold-up for each geometry of the diffuser. Cramers et al. [23] have investigated the effect of the gas density on the gas hold-up in ejector loop reactors. They have observed that the gas hold-up increases with gas density. They too have found a linear relationship between the gas hold-up and the superficial velocity of the entrained gas in agreement with the observations of [16,21,25] have reported the regimes developed and the importance of swirl bodies in the ejector. All the proposed correlations for the fractional gas hold-up are summarized in Table 3.

Table 3
Hold-up, $k_L a$ and a measurement methods and correlations given by various authors

System	Dimensions (m)	Q_G (m ³ /s)	Q_L (m ³ /s)	Method of measurement			Correlation	Author
				Hold-up	$k_L a$	a		
Upward, primary—water; secondary—air	$D_N = 0.006-0.016$, $D_T = 0.01-0.028$, $H_T = 0.05-0.26$	5×10^{-5} to 1.3×10^{-3}	0 to 6.6×10^{-4}	2,3			$\frac{\epsilon_G}{Q_G} = 0.5 \left(\frac{D_N}{D_T} \right)^{-0.3} F_G^{0.3}$, $\epsilon_{CO} = 0.38 U_G^{0.84}$, $U_G = \frac{Q_G}{\Delta P \rho_f / \mu^{1/4}}$	[15]
Upward, primary—water; secondary—air	Type 1: $D_N = 0.006-0.011$, $L = 0.025$ Type 2: $D_N = 0.006$, $L = 0.007$ Type 3: $D_N = 0.008$, $L = 0.0015$, $D_T = 0$, $H_T = 0$, $D_{Dist} = 0.0638$, $D_{Dist} = 0.159$, $H_D = 0.43$, $D_C = 0.292$ $D_N = 0.006-0.010$, $D_C = 0.292$	0.28×10^{-3} to 5.04×10^{-3}	0.5×10^{-3} to 2×10^{-3}	1	1		$\epsilon_G = 0.05 \frac{\rho_G}{D}$ $\epsilon_D = \frac{\Delta P Q_G}{V_L \rho_L}$ $k_L a = 0.04 \frac{\rho_G^{0.54}}{D}$	[16]
Upward, primary—water; secondary—air	$D_N = 0.008$, $D_T = 0.01$, $H_T = 0.225$, $D_C = 0.15$, $H_C = 1.795$	0.28×10^{-3} to 4.48×10^{-3} , $0.004-0.067$ m/s 0.1×10^{-3} m ³ /s	5.5×10^{-4} to 1.8×10^{-3} m ³ /s $0.6-67 \times 10^{-4}$ m ³ /s	1	1		$\epsilon_G = 3.47 U_G$, $k_L a = 2 U_G$	[17]
Upward, primary—water; secondary—air	$D_N = 0.008$, $L = 0.025$, 0.007 , 0.0015 , $D_{Dist} = 0.016$, $D_{Dist} = 0.04$ and 0.028 , $H_D = 0.1-0.4$, $D_C = 0.3$ m	8.3×10^{-4} to 7.7×10^{-3} m ³ /s, superficial velocity $0.013-0.107$ m/s	5.5×10^{-4} to 1.8×10^{-3} m ³ /s	1	1		$\epsilon_{G, Spout} = 0.346 U_G^{0.55} F_G^{0.3}$, $\epsilon_{G, Calm} = 0.346 U_G^{0.55} F_G^{0.3}$, $0.472 \times 10^{-2} < U_G < 5.6 \times 10^{-2}$ m/s, $D_N = 1.213 \times 10^{-2} U_G^{0.2} F_G^{-0.375}$, $k_L a_{Spout} = 8.42 \times 10^{-2} U_G^{0.6} F_G^{1.0}$, $k_L a_{Calm} = 0.329 U_G^{0.75} F_G^{0.55}$, $a_{Spout} = 0.285 U_G^{0.36} F_G^{0.8}$, $a_{Calm} = 0.249 U_G^{0.6} F_G^{0.65}$ $\epsilon_G = 0.057 U_G^n$, $n = 0.53$ (for $H_D = 0.4$), $n = 0.42$ (for $H_D = 0.2$), $n = 0.35$ (for $H_D = 0.1$), $k_L a = 0.036 U_G^{0.54}$	[18]
Upward, primary—water; secondary—air	$D_N = 0.008$, $L = 0.025$, 0.007 , 0.0015 , $D_{Dist} = 0.016$, $D_{Dist} = 0.04$ and 0.028 , $H_D = 0.1-0.4$, $D_C = 0.3$ m	8.3×10^{-4} to 7.7×10^{-3} m ³ /s, superficial velocity $0.013-0.107$ m/s	5.5×10^{-4} to 1.8×10^{-3} m ³ /s	1	1		$k_L a = 0.7 U_G^{0.58}$	[19]
Upward, primary—water; secondary—air	$D_N = 0.005$, 0.008 , 0.01 , 0.012 m, $D_T = 0.016$, 0.0159 m, $D_N/D_T = 1.6-3.2$	6.4×10^{-4} to 3.2×10^{-3} m ³ /s	4×10^{-4} to 2.8×10^{-3}	1			$\epsilon_G = A(Q_G)^B$, $A = 0.94-2.66$, $B = 0.74-1.54$	[10]
Downward, primary—water; secondary—air	$D_N = 0.0045$, 0.0065 m, $D_T = 0.018$ m, $D_C = 0.040$ m.	0.5×10^{-4} to 3.0×10^{-3}	1×10^{-4} to 5×10^{-4}	3	2		$k_L a = 0.044 \left(\frac{D_N}{D_T} \right)^{0.76}$	[9]
Downward, primary—solution of NaHCO ₃ and Na ₂ CO ₃ ; secondary—air + CO ₂ mixture	$D_N = 0.003-0.02$, $D_T = 0.01-0.03$, $H_T = 0.05-1.25$	0.25×10^{-3} to 1×10^{-4}	0.3×10^{-3} to 4×10^{-3}	2	1		$a_{Spout} = 15,000 U_G^{1.2}$, $a_{Calm} = 7500 U_G^{1.1}$	[21]
Upward, primary—sodium sulfite solution, secondary—air	$D_N = 0.004-0.006$, $D_T = 0.012$, $D_D = 0.04$	0.9×10^{-4} to 0.24×10^{-2}	0.3×10^{-3} to 0.8×10^{-3}	1			$\frac{k_L a \rho_G^{1/3}}{D_C} = 5.4 \times 10^{-4} Re^2 \frac{\rho_G}{\sigma^{1/3}}$, $1.3 < \frac{\rho_G}{\sigma} < 3$, $\frac{k_L a \rho_G^{1/3}}{D_C} = 3.1 \times 10^{-4} Re^2$	[22]
Downward, primary—water; secondary—air	Not mentioned	0.7×10^{-3}	2.8×10^{-4} to 2×10^{-3}	1			$\epsilon_G = 7.7 U_G \left(\frac{D_N}{D_T} \right)^{0.11}$	[23]
Downward, primary—water; secondary—air	$D_N = 0.009$	2.22×10^{-4} to 3.36×10^{-3}	5.56×10^{-4} to 2.22×10^{-3}	1			$a = 19,500 \left(\frac{D_N}{D_T} \right)^{0.4} \epsilon_G (1 - \epsilon_G)^{0.4}$	[24]
Upward, primary—water; secondary—air	$D_N = 0.006-0.012$, $D_T = 0.016$, $D_{Dist} = 0.04$	2.78×10^{-4} to 5.1×10^{-3}	5.5×10^{-4} to 2×10^{-3}	2			$\epsilon_G = 2.81 U_G^{0.9}$	[2]
Upward, primary—water; secondary—air	$D_N = 0.01$, $D_T = 0.018$, $H_T = 0-0.36$	0.233×10^{-3}	$0-0.083$ m/s	2			$\frac{\epsilon_G}{1 - \epsilon_G} = 5.91 U_G^{1.08} \frac{\rho_G^{0.03}}{D}$	[25]
Downward, primary—water; secondary—air	$D_N = 0.004$, 0.0047 and 0.0053 , $D_T = 0.012$, $H_T = 0.024-0.120$	$Q_G/Q_L = 0-1.5$	Not mentioned	1			$k_L a =$ $C_G^{0.65} \epsilon_G^A \left(\frac{\rho_G}{\sigma} \right)^{0.3} \left(\frac{H_T}{D_T} \right)^{0.42} \left[1 - 0.55 \left(0.38 - \frac{D_N}{D_T} \right)^2 \right]$	[1]

Table 3 (Continued)

System	Dimensions (m)	Q_G (m ³ /s)	Q_L (m ³ /s)	Method of measurement			Correlation	Author
				Hold-up	$k_L a$	a		
Downward, primary—water, CMC; secondary—air	$D_N = 0.004-0.008$, $D_T = 0.019$, $H_T = 0.184$, $H_D = 0.204$, $D_C = 0.0156$	1.11×10^{-6} to 1.89×10^{-5}	9.56×10^{-6} to 2.75×10^{-5}	2			$\epsilon_G = 0.365 Re^{-0.164} \left(\frac{D_N^A}{\sigma^{0.2}} \right)^{-0.029} A^{0.032} H_D^{0.207}$	[26]
Downward, primary—water; secondary—air	$D_N = 0.004-0.008$, $D_T = 0.019$, $H_T = 0.184$, $H_D = 0.204$	0.83×10^{-4} to 1.58×10^{-3}	0.98×10^{-4} to 2.63×10^{-4}	3	2		$k_L a = 1.08 U_G^{0.92}$, $a = 0.38 \times 10^4 U_G$	[27]

The fractional gas hold-up is a very strong function of the gas entrainment rate and this is reflected by the correlations proposed [10], which shows, $\epsilon_G \propto V_G^{0.794}$ and [23], which shows $\epsilon_G \propto V_G$.

The difference in the exponent with respect to power consumption for the two diffusers investigated by ref. [9] is very small.

1.3 Mass Transfer Characteristics

A number of physiochemical methods have been reported in the literature for the estimation of volumetric mass transfer coefficient ($k_L a$) of a multiphase contactor. Physical absorption of a solute gas in a liquid, chemical absorption of oxygen in aqueous solutions of sodium sulfite and chemical absorption of carbon dioxide in $\text{Na}_2\text{CO}_3\text{-NaHCO}_3$ solutions are commonly used for the determination of volumetric mass transfer coefficient [9,27]. For the estimation of interfacial area, chemical absorption of oxygen in aqueous sodium sulfite solutions and absorption of CO_2 in aqueous sodium hydroxide solution are the commonly used systems. Table 3 shows the geometry of ejectors used, methods of mass transfer coefficient ($k_L a$) and interfacial area (a) measurements and the correlations obtained by previous authors. Zahradnik et al. [17] has shown that the mass transfer coefficient in a bubble column operated with an ejector gas distributor increased linearly with the superficial velocity of the entrained gas ($k_L a = 2.0V_G$). However, the mass transfer characteristics for a conventional bubble column operated with a sieve plate distributor can be correlated as $k_L a = 0.75V_G^{0.85}$. It has been reported that the comparison of the two distributors shows that for the same mass flow rate, the ejector distributor gives higher mass transfer coefficients. Moresi et al. [28] investigated the performance of a fermentor operated with an ejector. They have correlated the values of mass transfer coefficient empirically with the power consumption per unit mass of the liquid. The values of mass transfer coefficient with 6 and 4mm diameter nozzles were not significantly different. Dutta and Raghavan [9] have empirically correlated the values of mass transfer coefficients in ejector loop reactors with the power consumption per unit volume of the reactor. Dirix and van der Wiele [22] have shown that there are two regimes in the ejectors namely the bubble (froth) flow regime and jet flow regime. In the bubble (froth) flow regime, the mass transfer coefficient depends on gas and liquid flow rates and also Reynolds' number (calculated from the fluid properties at the nozzle tip), whereas, in the jet flow regime it depends only on the nozzle Reynolds' number. Cramers et al. [23] have correlated the interfacial area with the jet power and the gas velocity. They have reported that the liquid height in the holding tank affects the mass transfer characteristics of the ejector significantly. The overall specific interfacial area increases with both the gas and liquid flow rates. At the lower gas flow rates, the gas holdup and the specific interfacial area are almost

proportional to the superficial gas velocity. For the higher liquid flow rates, this linear dependency vanishes abruptly caused by the change in the flow regime. It was shown by these authors that the ratio of D_N/D_T has a significant effect on the local energy dissipation rate within the mixing zone and consequently on the local k_L and a values. An optimum value of interfacial area was obtained for D_N/D_T of 0.4. Cramers and Beenackers [1] have reported a correlation for interfacial area as a function of the gas and liquid physical properties, specific power input and the gas hold-up. The reported correlations for volumetric mass transfer coefficients and interfacial area appear to depend significantly on the geometry of the ejector and power input per unit volume. It is worth to re-emphasize that all these correlations were developed for liquid as the motive fluid and gas as the entrained fluid. These models cannot be directly used for the present system where air is the motive fluid. Since the literature of ejectors with gas as a motive fluid is scanty, it was thought desirable to investigate the hydrodynamic and mass transfer characteristics of ejectors with air as a primary fluid with the help of detailed experiments.

II. Description of the Model

A high-pressure fluid (motive fluid) with very low velocity at the primary inlet is accelerated to high velocity jet through a converging nozzle for the liquid jet pump or a converging-diverging supersonic nozzle for the gas ejector. The supply pressure at the inlet is partly converted to the jet momentum at the nozzle exit. Thus the high velocity, low static pressure primary jet induces a secondary flow (propelled fluid) from the inlet or suction port and accelerates it in the direction of the driving jet. The two streams then combine in the mixing section, and ideally the process is complete by the end of this section. A diffuser is usually installed at mixing chamber exit to lift the static pressure of mixed flow. In the present model, the geometry at the throat and the diffuser is modified to constant rate of momentum change method and a pump is used to increase the velocity of the primary stream at the inlet. This reduces the momentum difference during mixing and in turn reduces the kinetic energy losses. The schematic view of the present model is shown in Fig.1. Based on the present model, an efficiency comparison is made to compare the small and large momentum differences between the motive and propelled streams.

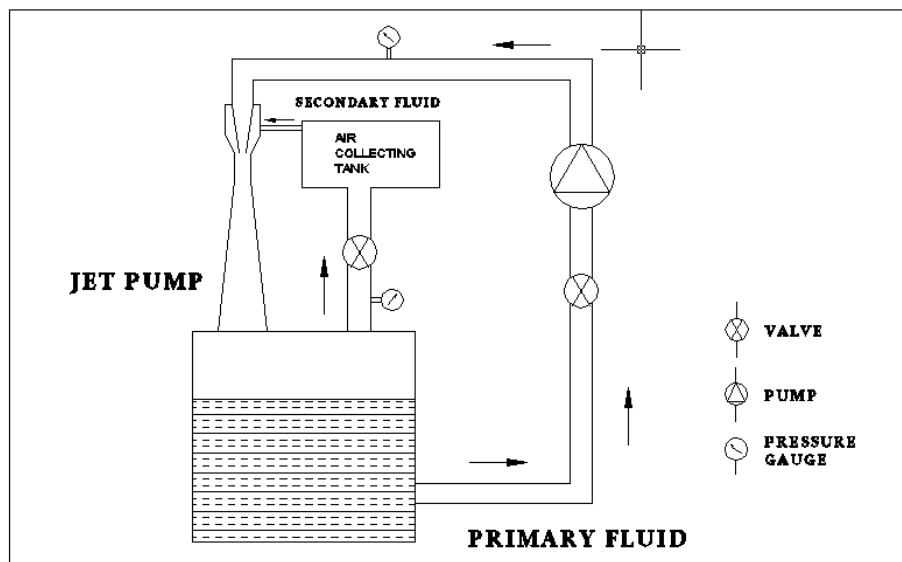


Figure 1(a): Description of the Model

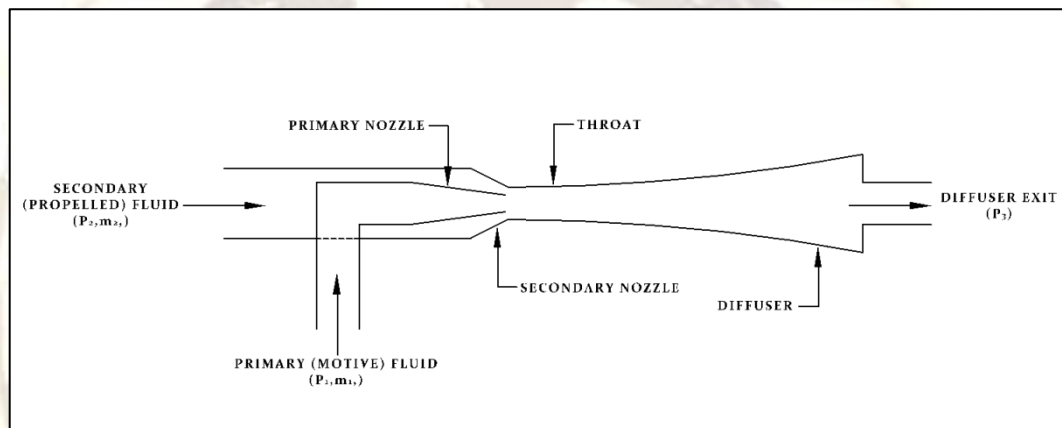


Figure 1(b) Enlarged View of Jet Ejector

III. CFD Modelling

Recently, with the rapid development of numerical solution methods, some researchers have attempted to apply computational fluid dynamics (CFD) in modeling the flow inside ejectors. Riffat and Omer [16] used a commercial CFD package to predict the performance of a methanol-driven ejector. Unfortunately, the results were not validated through any experimental data. Choi et al. [17] investigated numerically the flow of subsonic/sonic ejector of a bleed pump. Rusly et al. [18] simulated the flow through ejector used in cooling system. Sriveerakul et al. [19] investigated the performance of steam ejector used in a refrigeration system. Although there are numbers of papers that have investigated the ejector numerically using CFD, most of them did two-dimensional modeling. In this case, the CFD analysis could not account for the effect of three-dimensional flow phenomena in the suction chamber and in a part of the mixing tube where the mixing phenomena occur. In this study, a CFD package (Fluent 6.3) is employed to analyze a small water jet air ejector

which is equipped in an experimental mixing loop reactor. The ejector is modeled in two-dimensional geometry in order to get better agreement between simulation results and the real conditions. The effect of operating conditions and geometries on its hydrodynamics and mass transfer characteristics are investigated and validated with actual values obtained from experiment. In this research, five different models of ejector were developed to investigate the influence of mixing tube length on the mass transfer characteristics. The ejector geometry is modeled on a commercial software package Gambit software is employed for generating grid and CFD solver.

3.1 Geometries and Grids

As proposed, Gambit software package was used to create the calculation domain and grid elements of the model. The mesh and model were created in a three-dimensional (3D) domain to account for the local details of the complex flow structure taking place during ejector operation. The geometries of the calculation domain of the modeled

gas-liquid ejectors are described. For preliminary results, the grid was initially made of about 100,000 structured trimmed quadrilateral cells with variation of sub layer thickness to accommodate the curving nature and sharp angle of the ejector geometries as shown in Figure 2. The concentration of grid density is focused on the areas where significant phenomena are expected. In order to obtain the grid independent

result, reasonable numbers of iterations were conducted by refining the mesh in every stage of simulation. After several simulations, the fixed number of cells with grid-independent result was obtained as 395,240 cells. In this study, the grid cell volume used in the CFD simulation of ejector was set for about 400,000 cells.

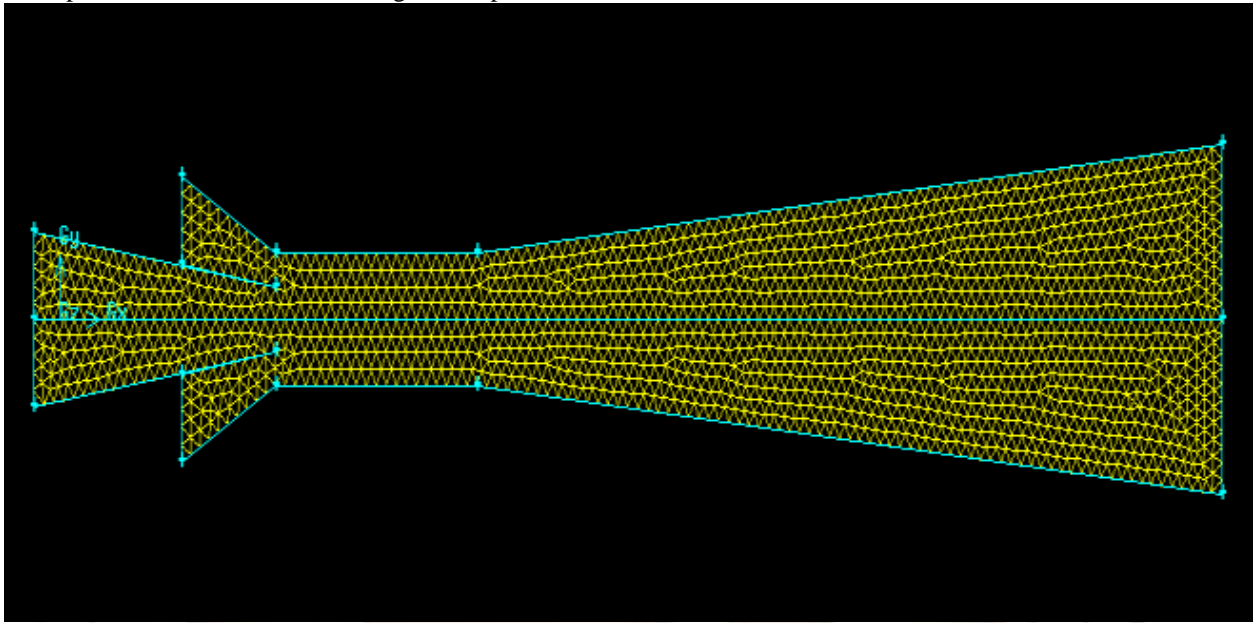


Figure 2 Meshed Model of Jet Ejector

3.2 Case setup

As the working fluids used in this research are water as primary fluid and air as secondary fluid, so the assumption of incompressible flow is appropriate. Hence, the *standard k-ε* with high Reynolds number is selected to govern the turbulence characteristics. The near wall treatment was left as the *standard wall function*, which gives reasonably accurate results for the wall bounded with very high Reynolds number flow. The thermo physical properties of the working fluids were obtained at 293 K and 300 K, respectively, for water and air. The turbulence intensity was set to be 3.5% for primary fluid.

3.3 Boundary conditions

Boundary conditions of two faces entering a primary nozzle and ejector were set as velocity inlet and pressure inlet, respectively. The face at the exit of ejector was set as outlet boundary. At the inlet boundary, the velocity components, turbulent kinetic energy and turbulent dissipation rate have to be

specified. The applied velocity at the inlet boundary was based on the experimentally measured volumetric flow rate, which was 4 m³/h of water. The velocity of air was based on the Q_G/Q_L ratio in the

range of 0.2 to 1.2. This ratio was selected in order to maintain bubbly flow regimes inside the ejector.

3.4 Calculation of volumetric mass transfer coefficient

Based on their experimental results, Dirix and van de Wiele [22] recommend empirical correlations for mass transfer coefficient on the liquid side for a down flow ejector as

$$k_L a = 5.4 \times 10^{-3} (\epsilon)^{0.66} \epsilon_G \left(\frac{d_M}{d_D} \right)^{0.66} \quad (1)$$

$$k_L a = 8.5 \times 10^{-4} (\epsilon)^{0.66} \left(\frac{d_M}{d_B} \right)^{0.66} \quad (2)$$

Where,

$$\epsilon_G = \frac{Q_G}{Q_G + Q_L} \quad (3)$$

Eq. (1) is used to calculate the volumetric mass transfer coefficient of the ejector in the bubbly flow regimes. Meanwhile, Eq. (2) is used for the jet flow regimes inside the ejector. In this research, Eq. (1), (2), and (3) will be used for the analysis of

hydrodynamics and mass transfer characteristics in the ejector.

IV. Results and Discussion

The simulated results have helped in understanding the local interactions between the two fluids, and recompression rate which in turn made it possible for a more reliable and accurate geometric design and operating conditions. Many numerical studies about supersonic ejectors have been reported since 1990s in predicting ejector performance and providing a better understanding of the flow and mixing processes within the ejector (Riffat et al, Ouzzane & Aidoun, Alexis & Rogdakis, Chunnanond & Aphornratana, pump (Beithou & Aybar) and in mixing processes (Arbel et al

). The jet ejectors are designed for $ER = 1$. Fluent simulation shows that the jet ejector designed based on conventional method produces an $ER = 0.57$, whereas high efficiency jet ejector produces an $ER = 0.73$. In conventional jet ejector there is drop in ER since shock wave occurs at the end of constant area mixing chamber. Fig. 3 shows the static pressure along the axis of the jet ejector. The presence of shock wave increases the static pressure. Since shock wave generation is an irreversible process, there is drop in efficiency of jet ejector. CRMC method eliminates the formation of shock wave in the mixing area. The cross sectional area of the mixing region of jet ejector is not constant. The mixing region and diffuser are replaced by a convergent and divergent diffuser.

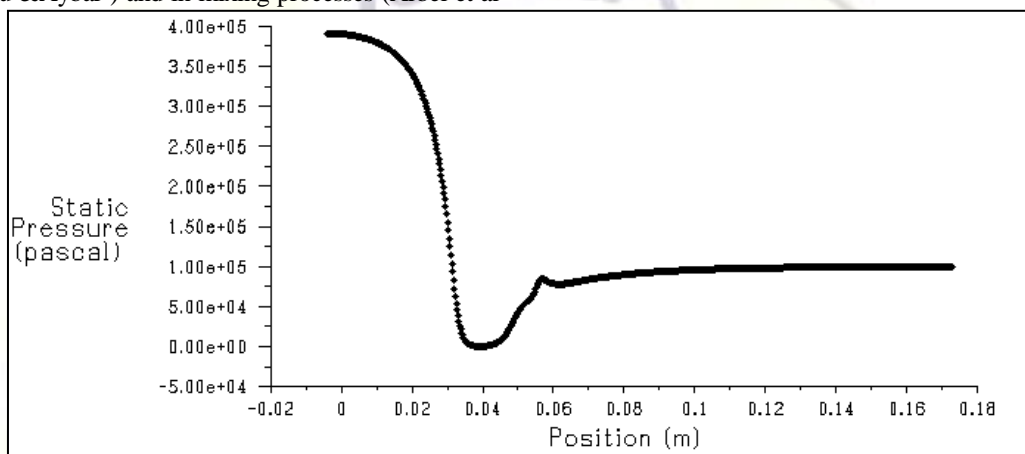


Figure 3: Static Pressure along the Axis of High Efficiency Jet Pump

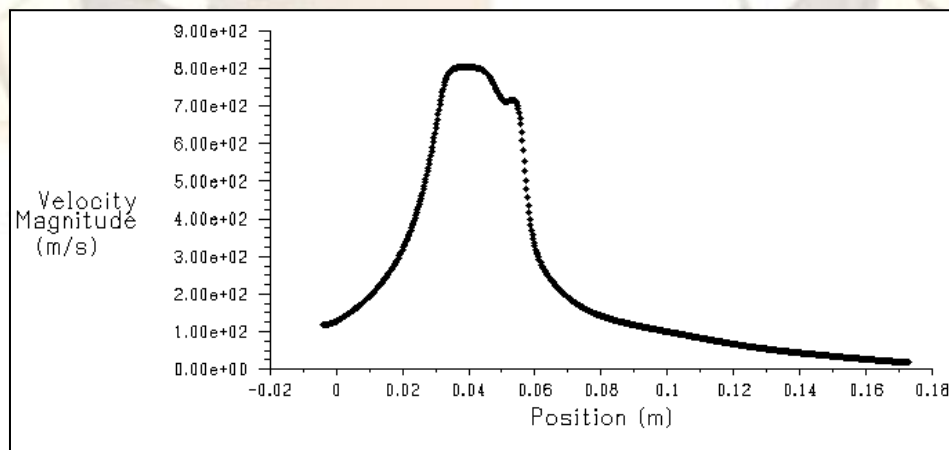
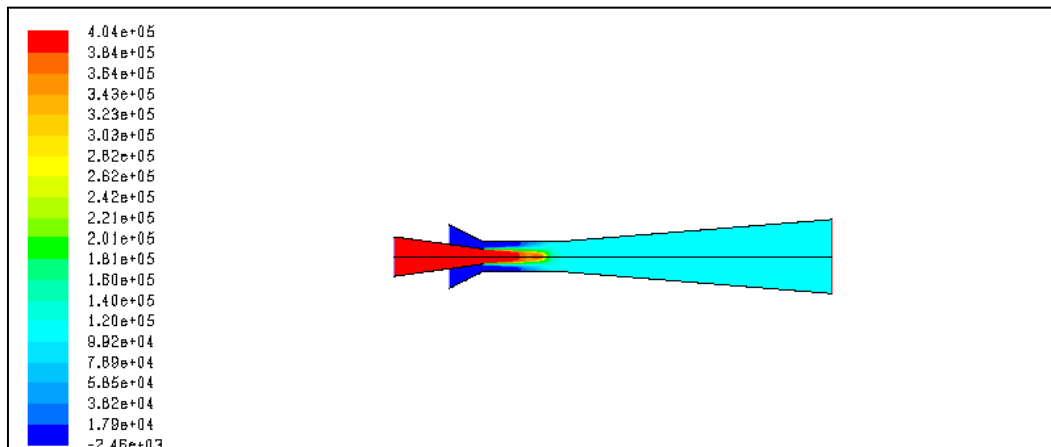


Figure 4: Velocity Magnitude along the Axis of High Efficiency Jet Pump

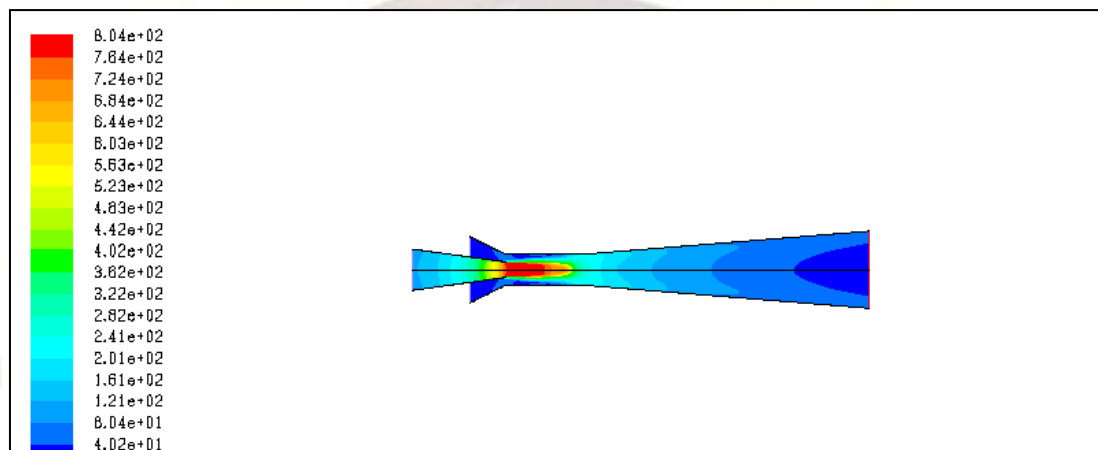
Figure (5) shows the pressure and velocity contour map inside the jet pump with conventional model. It is seen from the contour plot that the maximum

flow velocity occurs at the exit of the primary nozzle of the compressor, after which the velocity decreases because of exchange of momentum and mixing with the secondary fluid stream. It is also observed that due to the

boundary layer effect a velocity gradient is observed from the wall to the centre line flow of the jet compressor. The view shows the conversion of pressure energy to kinetic energy as the flow becomes supersonic. At the throat, due to momentum exchange with the secondary fluid the flow becomes almost sonic. Further, in the diffuser section the remaining kinetic energy is converted to pressure energy.



(a) Pressure Contour for High Efficiency Jet Pump



(b) Velocity Contour for High Efficiency Jet Pump

Figure 5: Pressure, Velocity Contours of High Efficiency Jet Pump

V. Conclusions

In the present work, hydrodynamic characteristics of ejectors using water as the motive fluid and air as the entrained fluid have been investigated. A semiempirical model has been developed to predict the performance of the ejector. The model predictions have been found to be in good agreement with the experimental measurements. The effects of ejector geometry and operating conditions on the liquid entrainment have been explained on the basis of the model developed in terms of the pressure drop and the driving force. A CFD model is developed to elucidate the hydrodynamics characteristics of an ejector. The model was first validated by varying the primary fluid flow rate, and then the inlet pressure, suction pressure and outlet pressure were calculated. The CFD results have a good agreement with experimental data. The CFD result also matches the

experimental data very well increase of gas-liquid flow rate ratio results in a reduction of the volumetric mass transfer coefficient.

REFERENCES

- [1] P.H.M.R. Cramers, A.A.C.M. Beenackers, Influence of the ejector configuration, scale and the gas density on the mass transfer characteristics of gas-liquid ejectors, *Chem. Eng. J.* 82 (2001) 131–141.
- [2] J. Zahradnik, M. Fialova, V. Linek, J. Sinkule, J. Renickoca, F. Kastanek, Dispersion efficiency of ejector-type gas distributors in different operating modes, *Chem. Eng. Sci.* 52 (24) (1997) 4499–4510.
- [3] P. Havelka, V. Linek, J. Sinkule, J. Zahradnik, M. Fialova, Hydrodynamics and mass transfer characteristics of ejector loop reactors, *Chem. Eng. Sci.* 55 (2000) 535–549.
- [4] D.K. Acharjee, P.A. Bhat, A.K. Mitra, A.N. Roy, Studies on momentum transfer in vertical liquid jet ejectors, *Indian J. Technol.* 13 (1975) 205–210.
- [5] A. Ben Brahim, M. Prevost, R. Bugarel, Momentum transfer in a vertical down flow liquid jet ejector: case of self gas aspiration

- and emulsion flow, *Int. J. Multiphase Flow* 10 (1) (1984) 79–94.
- [6] S.M. Dave, H.M. Sadhukhan, O.A. Novaro, *Heavy Water*, Quest publications, Mumbai, India, 1997.
- [7] G.S. Davies, A.K. Mitra, A.N. Roy, *Momentum transfer studies in ejectors*, *Ind. Eng. Chem. Process Des. Dev.* 6 (3) (1967) 293–299.
- [8] P.A. Bhat, A.K. Mitra, A.N. Roy, *Momentum transfer in a horizontal liquid jet ejector*, *Can. J. Chem. Eng.* 50 (1975) 313–317.
- [9] N.N. Dutta, K.V. Raghavan, *Mass transfer and hydrodynamic characteristics of loop reactors with down flow liquid jet ejectors*, *Chem. Eng. J.* 36(1987) 111–121.
- [10] S.R. Bhutada, V.G. Pangarkar, *Gas induction and hold-up characteristics of liquid jet loop reactors*, *Chem. Eng. Commun.* 61 (1987) 239–261.
- [11] M.N. Biswas, A.K. Mitra, *Momentum transfer in horizontal multi-jet liquid–gas ejector*, *Can. J. Chem. Eng.* 59 (1981) 634–637.
- [12] H. Henzler, *Design of ejectors for single phase material systems*, *Germ. Chem. Eng.* 6 (1983) 292–300.
- [13] R.G. Cunningham, *Gas compression with the liquid jet pump*, *Trans ASME—J. Fluids Eng.* 96 (1974) (1974) 203–215.
- [14] M. Mandal, G. Kundu, D. Mukherjee, *Energy analysis and air entrainment in an ejector induced down flow bubble column with Non-Newtonian motive fluid*, *Chem. Eng. Technol.* 28 (2) (2005) 210–218.
- [15] T. Otake, S. Tone, R. Kuboi, Y. Takahashi, K. Nakao, *Dispersion of a gas by a liquid jet ejector*, *Int. Chem. Eng.* 21 (1981) 72–80.
- [16] J. Zahradnik, J. Kratochvil, F. Kastanek, M. Rylek, *Energy effectiveness of bubble column reactors with sieve tray and ejector type gas distributors*, *Chem. Eng. Commun.* 15 (1982) 27–40.
- [17] J. Zahradnik, J. Kratochvil, F. Kastanek, M. Rylek, *Hydrodynamic characteristics of gas–liquid beds in contactors with ejector type gas distributors*, *Collect. Czech. Chem. Commun.* 47 (1982) 1939–1949.
- [18] S. Ogawa, H. Yamaguchi, S. Tone, T. Otake, *Gas–liquid mass transfer in the jet reactor with liquid jet ejector*, *J. Chem. Eng. Jpn.* 16 (1983) 419–425.
- [19] M. Rylek, J. Zahradnik, *Design of Venturi-tube gas distributors for bubble type reactors*, *Collect. Czech. Chem. Commun.* 49 (1984) 1939–1948.
- [20] J. Zahradnik, J. Kratochvil, M. Rylek, *Gas holdup and interfacial mass transfer in gas–liquid tower contactors with ejector type gas distributors*, *Collect. Czech. Chem. Commun.* 50 (1985) 2535–2544.
- [21] Y. Bando, M. Kuraishi, M. Nishimura, I. Takeshita, *The characteristics of a bubble column with a gas-suction type, simultaneous gas–Liquid injection nozzle*, *Int. Chem. Eng.* 30 (1990) 729–737.
- [22] C.A.M.C. Dirix, K. van derWiele, *Mass transfer in jet loop reactors*, *Chem. Eng. Sci.* 45 (1990) 2333–2340.
- [23] P.H.M.R. Cramers, L.L. van Dierendonck, A.A.C.M. Beenackers, *Influence of the gas density on the gas entrainment rate and gas hold-up in loop venturi reactors*, *Chem. Eng. Sci.* 47 (1992) 2251–2256.
- [24] P.H.M.R. Cramers, L.L. van Dierendonck, A.A.C.M. Beenackers, *Hydrodynamics and mass transfer characteristics of a loop venturi reactor with a downflow liquid jet ejector*, *Chem. Eng. Sci.* 47 (1992) 3557–3564.
- [25] P. Havelka, V. Linek, J. Sinkule, J. Zahradnik, M. Fialova, *Effect of the ejector configuration on the gas suction rate and gas hold-up in ejector loop reactors*, *Chem. Eng. Sci.* 52 (1997) 1701–1713.
- [26] A. Mandal, G. Kundu, D. Mukherjee, *Gas holdup and entrainment characteristics in a modified downflow bubble column with Newtonian and non-Newtonian liquid*, *Chem. Eng. Process.* 42 (2003) 777–787.
- [27] A. Mandal, G. Kundu, D. Mukherjee, *Interfacial area and liquid-side volumetric mass transfer coefficient in a downflow bubble column*, *Can. J. Chem. Eng.* 81 (2003) 212–219.
- [28] M. Moresi, G.B. Gianturco, E. Sebastiani, *The ejector-loop fermenter: description and performance of the apparatus*, *Biotechnol. Bioeng.* 25 (12)(1983) 2889–2904.
- [29] U. ParasuVeera, J.B. Joshi, *Measurement of gas hold-up profiles by Gamma Ray Tomography: effect of sparger design and height of dispersion in bubble columns*, *Trans. Inst. Chem. Eng.* 77A (1999) 303–315.
- [30] A.R. Thatte, R.S. Ghadge, A.W. Patwardhan, J.B. Joshi, G. Singh, *Local hold-up measurements in sparged and aerated tanks by γ -ray attenuation technique*, *Ind. Eng. Chem. Res.* (2004) 5389–5399.
- [31] L.K. Doraiswamy, M.M. Sharma, *Heterogeneous Reactions: Analysis, Examples and Reactor Design*, vol. 2, Wiley Interscience, New York, 1983.

- [32] P.V. Danckwerts, Gas-Liquid Reactions, McGraw Hill, New York, 1970.
- [33] P.V. Danckwerts, M.M. Sharma, Chemical methods for measuring interfacial areas and mass transfer coefficients in two-fluid systems, Br. Chem.Eng. 15 (1970) 522-528.
- [34] C.E. Lapple, Isothermal and adiabatic flow of compressible fluids, Trans.AIChEngers.39 (1943) 385.
- [35] O. Levenspiel, The discharge of gases from a reservoir through a pipe, AIChE J. 23 (8) (1977) 403-404.
- [36] W.J. Davis, The effect of the Froude number in estimating vertical twophase gas-liquid friction factor, Br. Chem. Eng. 8 (7) (1963) 462-465.
- [37] M.T. Kandakure, V.G. Gaikar, A.W. Patwardhan, Hydrodynamic aspects of ejectors, Chem. Eng. Sci. 60 (2005) 6391-6402.
- [38] G.B. Tatterson, Fluid Mixing and Gas Dispersion in Agitated Vessels, McGraw Hill, New York, 1991.
- [39] W.D. Deckwer, Bubble Column Reactors, Wiley, New York, 1992.

